2016

Radiative property characterization of spherical void phase graphitic foam with application to solar collection

Nolan J. Dyck
Western University

Anthony G. Straatman
uwo, agstraat@uwo.ca

International Journal of Heat and Mass Transfer 92 (2016) 1201–1204

Contents lists available at ScienceDirect

International Journal of Heat and Mass Transfer

journal homepage: www.elsevier.com/locate/ijhmt

Radiative property characterization of spherical void phase graphitic foam

Nolan J. Dyck, Anthony G. Straatman *

Department of Materials and Mechanical Engineering, Western University, 1151 Richmond St., London, Ontario, Canada

ARTICLE INFO

Article history:
Received 5 December 2014
Received in revised form 21 September 2015
Accepted 22 September 2015

Keywords:
Radiation
Porous media
Graphitic foam
Monte-Carlo method

ABSTRACT

The present work uses a popular discrete-scale Monte-Carlo method to determine the extinction coefficient of spherical-void-phase graphitic foams having mean pore diameters $d \in \{400\ \mu m, 600\ \mu m, 800\ \mu m\}$, with porosities $\varepsilon \in \{0.70, 0.75, 0.80, 0.85\}$. The representative elementary volumes were constructed using a digital generation method, and the surface-area-to-volume ratios were identified directly from the digital models. The extinction coefficients were identified using the aforementioned method and a correlation is fitted to the data. It was found that the extinction coefficient is very large, suggesting that, for mean pore diameters and porosities in the given ranges, graphitic foam may nearly always be treated as a black body.

1. Introduction

Many engineering applications involve radiation transport within porous materials, including porous burners [1–3], and solar collectors [4,5]. If the volume-averaged radiative properties (absorption and scattering coefficients) of the porous structure are known, the Radiation Transfer Equation (RTE) may be applied to obtain the radiation field within the domain. Appropriate source and sink terms may be added to the RTE and the energy equation to enable the two-way coupling required to solve a wide variety of engineering problems.

A common method for determining radiation properties in heterogeneous media is the Monte Carlo (MC) ray-tracing technique originally presented by Tancrez and Taine [6]. Variations of the method have also been proposed by Petrash et al. [7] and Coquard and Baillis [8]. The method requires that a large number of ray-bundles be launched from non-opaque phases within a representative microstructure. The ray-bundles are allowed to interact naturally at phase boundaries as they propagate through the media. The histories of the ray-bundles are fitted to appropriate statistical distribution functions, and the best fit coefficients are identified as the pertinent effective properties. Researchers have successfully implemented this method to obtain radiative properties in idealized geometries [6,8,9], as well as real microstructures [9–11], where the digital approximation of the physical sample is obtained through X-ray tomography.

In an earlier work, a method for obtaining digital samples of porous media from aggregate statistical data was described, and digital samples of graphitic foam were produced to validate and demonstrate the method [12]. The present work employs the same method to generate digital samples of graphitic foam, and a discrete-scale MC ray-tracing technique is applied to those samples to determine extinction coefficients.

2. Radiation property identification

As mentioned above, the MC ray-tracing technique has been successfully used to determine the radiation properties of a variety of porous media. The reasoning behind the method introduced by Tancrez and Taine [6] will be reviewed here, followed by a brief description of the present implementation, and discussion of the results.

2.1. Bouger's law and the cumulative distribution function

The derivation begins with the definition of the extinction coefficient. Consider the incident radiation impinging normally on a slab of semi-transparent material of infinitesimal thickness, as in Fig. 1.

It has been experimentally observed that radiation within such a slab is attenuated in accordance with the proportionality

* Corresponding author. Tel.: +1 (519) 661 2111x88249.
E-mail address: astraatman@uwo.ca (A.G. Straatman).

http://dx.doi.org/10.1016/j.ijheatmasstransfer.2015.09.065
0017-9310/

Nomenclature

a_n	polynomial fit coefficient
A	interfacial surface area per unit volume of a porous sample
d	bubble diameter
F	separating force between bubbles in contact
$G(z)$	cumulative distribution function; fraction of rays attenuated before depth z
I	intensity of radiation
N, N_o, N'_z	number of photons (rays)
N_s	number of primitives within the sample
R_{AVG}	$\frac{R_1+R_2}{2}$ average bubble radius of a pair of bubbles in contact
z	Cartesian co-ordinate
β	extinction coefficient
β^+	non-dimensional extinction coefficient
ΔD	overlap or penetration distance between bubbles in contact
σ_t	surface tension coefficient

$$dI \propto -Idz \tag{1}$$

Inserting the extinction coefficient, β, into proportionality (1) and solving the resulting differential equation results in

$$I = I_o e^{-\beta z} \tag{2}$$

Eq. (2) is Bouger's law, which is sufficient to describe the attenuation of radiation in many semi-transparent media. It is widely accepted that intensity in a particular direction is proportional to the number of photons traveling in that direction, therefore, Eq. (2) can be rewritten as

$$N = N_o e^{-\beta z} \tag{3}$$

where N_o is the number of photons entering the medium, and N is the number of photons leaving the slab. Eq. (3) can also be expressed in terms of the number of photons attenuated before reaching the thickness z, N'_z:

$$\frac{N'_z}{N_o} = 1 - e^{-\beta z} \tag{4}$$

Finally, the fraction of absorbed photons at distance z is identified as the cumulative distribution of photon travel distances, or ray lengths:

$$G(z) = 1 - e^{-\beta z} \tag{5}$$

Eq. (5) is accurate for many homogenous, semi-transparent media, and it is desirable to treat heterogeneous media in a similar manner. In a two-phase medium, such as graphitic foam, $G(z)$ can be empirically determined by casting a large number of rays from the transparent phase and analyzing each of their histories. $G(z)$ may be inserted into Eq. (5) to evaluate β.

2.2. Implementation of the MC ray-tracing method

Two key assumptions can be made to simplify the ray-casting procedure. If the geometry is considered homogenous at the macroscopic scale, the distribution of ray lengths will not vary with the position of the origin plane, so ray origins may be selected from all points within the fluid phase. Moreover, if the geometry is isotropic, a similar argument leads to the conclusion that ray directions may also be randomly selected.

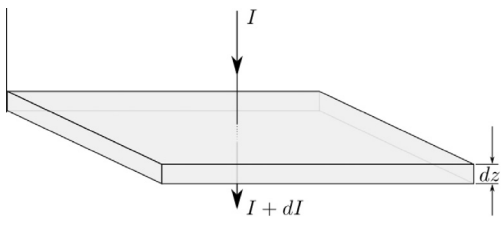

Fig. 1. Intensity incident normally on an attenuating slab of thickness dz.

In the present study, the graphitic foam under consideration has two distinct phases: the solid graphitic matrix, and the intervening fluid. Baillis et al. [13] have shown that the hemispherical reflectance of a 4.3 mm thick sample of carbon foam is less than 0.08% for incident wavelengths in the range $\lambda \in [0.2, 2]$ μm. Given this evidence we have assumed the solid matrix to be black, while the fluid of interest, air, is considered to be transparent. Only wavelength-averaged quantities will be considered in this work.

Rays are launched from random locations within the fluid phase in random directions. Upon collision with the solid matrix, the ray is terminated, and its cumulative length is calculated and written to file. When a collision is detected at the periodic boundary of the microstructure, the ray length is stored, and the ray relaunched in the same direction from the corresponding location on the opposite face. Since the samples are fully periodic, any ray intersecting a periodic boundary will continue to propagate in the fluid phase from the opposite face. Upon completion, a computer program was used to bin the ray lengths and fit the data to Eq. (5).

2.3. Digital sample generation

Before executing the discrete-scale MC technique to determine the desired properties, digital samples of the porous medium of interest must be produced. In the present work, these are generated using the method described by Dyck and Straatman [12], which is briefly summarized here.

Some two-phase media are best described as packings of particles, where the particles comprise the discrete phase. The opposite phase is usually a continuous substance in which the packing is immersed. To analyze such media using the aforementioned method, the analyst must choose a set of particle geometries to be packed into a periodic domain. The particles should be placed at random locations within an initial volume without interference. When all the particles have been inserted, the periodic walls of the domain are slowly compressed. During compression, contact between particles is resolved using a pre-determined force–displacement relationship, or contact law. The simulation is finished when a target criterion is reached (e.g. desired porosity has been achieved).

For the case of graphitic foam, the natural particle geometry is the sphere, which represents a bubble inside the domain. It is further assumed that the bubble diameters may be sampled from a normal distribution, whose mean and standard deviation are representative of the bubbles in the foam of interest. Distribution parameters such as the mean bubble diameter and standard deviation may be selected by the modeler. Bubble diameters remain constant during compression. The bubble–bubble contact law proposed by Dyck and Straatman [12] has been used:

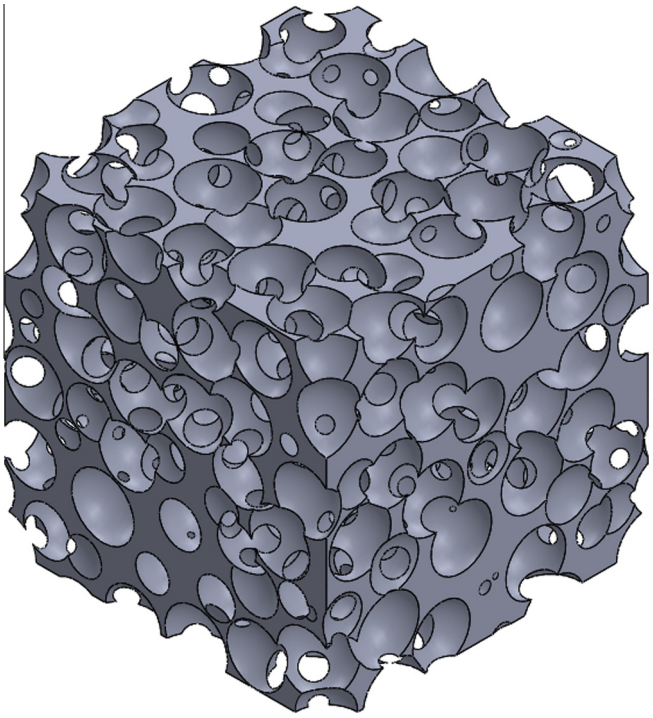

Fig. 2. Positive volume of a digitally generated graphitic foam sample; $N_s = 200$, $d = 400$ μm, $\sigma_d = 120$ μm, $\varepsilon = 0.80$.

$$\Delta D \cong \frac{F}{2\pi\sigma_t} \log\left(\frac{F}{8\pi\sigma_t R_{AVG}}\right) \tag{6}$$

where a suitable surface tension, $\sigma_t = 0.035$ N/m (see Ref. [14]), has been assumed. An image generated using Solidworks™ [15] of a typical digital sample can be seen in Fig. 2.

One of the aims of the present work is to determine the effects of varying porosity and mean bubble diameter on the overall extinction coefficient; however, before generating these samples, we must decide the number of rays to cast in each MC simulation, as well as a suitable Representative Elementary Volume (REV) size.

2.4. Number of rays

Before determining a suitable REV size, the number of rays which will be tracked in each MC analysis must be decided. If too few rays are tracked, the computed extinction coefficient will vary considerably between independent simulations, while tracking too many rays will require excessive computational resources. Given Tancrez and Taine's [6] decision to track 2×10^4 rays in each simulation involving samples of 100 primitives, we have decided to track 5×10^4 rays. Five independent MC analysis were run using a sample with the properties $N_s = 800$, $d = 400$ μm, $\sigma_d = 120$ μm, $\varepsilon = 0.80$. Between each of the five trials the predicted extinction coefficient remained within ±0.7% of the mean. Each simulation required approximately 2 min to complete on a workstation equipped with an Intel i5 CPU. Since both the variance of the results and the computation time were acceptable to us, we have decided to track 5×10^4 rays in each of the simulations described in this work.

2.5. REV sizing

When collecting data from small material samples, it is important to verify that the samples are indeed representative of the material of interest. Groups of small samples are expected to exhibit large variance in effective properties because they do not contain a statistically relevant number of microstructural features. Conversely, very large samples require more computational resources to generate and analyze. Any sample containing enough microstructural features to accurately predict the properties of interest is called a Representative Elementary Volume (REV). In the present work, it was of interest to determine a suitable REV size for extinction coefficient identification. To this end, a set of 24 cubic digital graphitic foam samples were generated; bubble diameters were sampled from a normal distribution with a mean, $d = 400$ μm, and standard deviation $\sigma_d = 120$ μm. Each sample contained between 100 and 800 primitives. The final porosity of each sample is $\varepsilon = 0.80$. The results for extinction coefficient from these cases can be seen in Fig. 3.

In Fig. 3, the data has no discernible trends, and are scattered about the mean value, $\beta^+ = 1.72$. Because all the data lie within ±2% of the mean, the number of rays cast was deemed sufficient for the present application, and all sample sizes appear to have a sufficient number of features to accurately predict the desired property. This analysis has given the authors confidence to assume that samples containing $N_s = 300$ bubbles will serve as adequate REVs for predicting radiative properties of graphitic foam for similar porosities and average bubble diameters.

2.6. Property identification

In the present study, it is of interest to see the effects of pore diameter and porosity variation on the extinction coefficient of graphitic foam. This section describes the property identification process.

To begin, three sets of REVs were generated with average bubble diameters, $d \in \{400\ \mu m, 600\ \mu m, 800\ \mu m\}$, and standard deviations, $\sigma_d \in \{120\ \mu m, 180\ \mu m, 240\ \mu m\}$, respectively. Each set contains 4 subsets whose porosities are $\varepsilon \in \{0.70, 0.75, 0.80, 0.85\}$. Each of these subsets contains 5 statistically similar REVs. Thus, the total number of REVs generated is $3 \times 4 \times 5 = 60$.

Discrete MC analyses were conducted using all REVs to predict effective extinction coefficients. At least 5×10^4 rays were launched from random locations and random directions from the fluid phase of each REV. The results can be seen in Fig. 4.

Fig. 4 shows the expected downward trend with increasing porosity. Note that the extinction coefficient has been scaled using the internal surface area per unit volume, A_{fs}, for comparison with Ref. [6]. Simply stated, a larger void fraction will allow rays to tra-

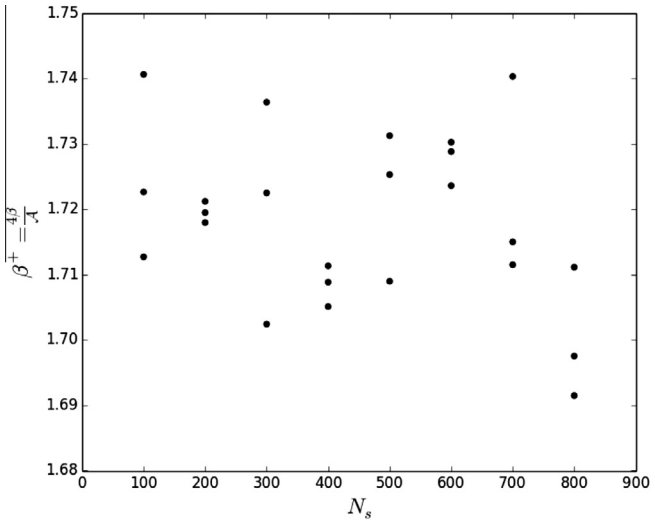

Fig. 3. Extinction coefficient vs. number of primitives. β^+ is the non-dimensional extinction coefficient.

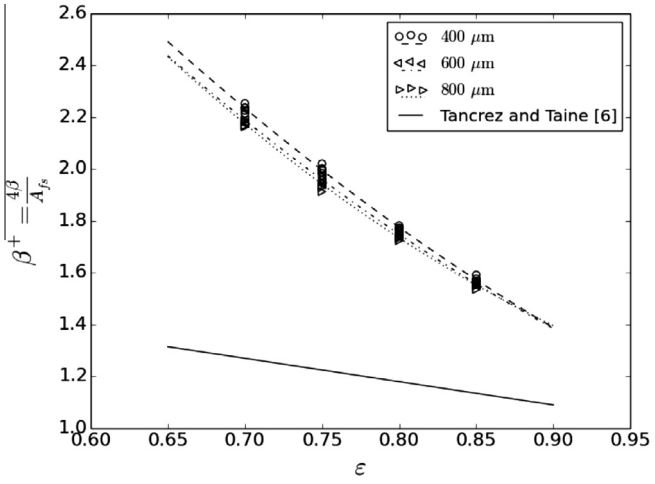

Fig. 4. Non-dimensional extinction coefficient vs. porosity.

Table 1
Summary of the polynomial coefficients applicable to Eq. (7).

d (μm)	a_0	a_1	a_2
400	3.61	−10.0	3.61
600	7.39	−10.1	3.79
800	8.12	−12.1	5.11

vel further before attenuation, resulting in a smaller extinction coefficient. The data also shows a weak, positive correlation with average pore diameter. While the samples are expected to yield the same results on average, there is an element of randomness in the generation and ray-casting processes.

Consequently, there are also small variations in the predicted properties — explaining why slightly different extinction coefficients are observed for statistically similar REVs. The data has been fitted by a second order polynomial of the form

$$\beta^+ = a_2\varepsilon^2 + a_1\varepsilon + a_0, \tag{7}$$

where the coefficients pertaining to each average diameter are given in Table 1.

Tancrez and Taine [6] have also employed this method to identify the non-dimensional extinction coefficient for the case of dispersed radius overlapping transparent fluid spheres where $\varepsilon \in [0, 1]$, and proposed the correlation $\beta^+ \approx 1 + 0.90(1-\varepsilon)$, which has been plotted in Fig. 4. The geometric structures used in that study are similar to the present geometries, with one distinction: the sphere centers in [6] were randomly placed inside the domain, whereas the spheres in Ref. [12] were packed together. Because the samples used to determine the present results are more physically accurate than those in [6], we believe our computed extinction coefficients are also more accurate. Furthermore, since it was found that the extinction coefficient is very large, for mean pore diameters and porosities in the given ranges, it is found that graphitic foam may nearly always be treated as a black body.

3. Summary

In the present work we have generated digital, statistically random REVs representing spherical-void-phase graphitic foams with differing mean pore diameters and porosities, and applied a statistical MC method to identify their effective extinction coefficients. It was found that the non-dimensional extinction coefficients were shown to have a strong, negative correlation with porosity, and a weak, positive correlation with mean pore diameter. The results have been satisfactorily fitted to a second order polynomial, which may be used to evaluate extinction coefficients in lieu of experimental data.

Conflict of interest

None declared.

Acknowledgment

The authors gratefully acknowledge the financial support received from the Natural Sciences and Engineering Research Council of Canada (NSERC).

References

[1] J.R. Howell, M.J. Hall, J.L. Ellzey, Combustion of hydrocarbon fuels within porous inert media, Progress in Energy and Combustion Science 22 (2) (1996) 121, http://dx.doi.org/10.1016/0360-1285(96)00001-9 (Available: <http://www.sciencedirect.com/science/article/pii/0360128596000019>).
[2] A.J. Barra, G. Diepvens, J.L. Ellzey, M.R. Henneke, Numerical study of the effects of material properties on flame stabilization in a porous burner, Combust. Flame 134 (4) (2003) 369, http://dx.doi.org/10.1016/S0010-2180(03)00125-1 (Available: <http://www.sciencedirect.com/science/article/pii/S0010218003001251>).
[3] A.J. Barra, J.L. Ellzey, Heat recirculation and heat transfer in porous burners, Combust. Flame 137 (1–2) (2004) 230, http://dx.doi.org/10.1016/j.combustflame.2004.02.007 (Available: <http://www.sciencedirect.com/science/article/pii/S0010218004000537>).
[4] S. Singh, P. Dhiman, Thermal and thermohydraulic performance evaluation of a novel type double pass packed bed solar air heater under external recycle using an analytical and RSM (response surface methodology) combined approach, Energy 72 (2014) 344, http://dx.doi.org/10.1016/j.energy.2014.05.044 (Available: <http://www.sciencedirect.com/science/article/pii/S0360544214006100>).
[5] P. Dhiman, N.S. Thakur, S.R. Chauhan, Thermal and thermohydraulic performance of counter and parallel flow packed bed solar air heaters, Renewable Energy 46 (2012) 259–268, http://dx.doi.org/10.1016/j.renene.2012.03.032.
[6] M. Tancrez, J. Taine, Direct identification of absorption and scattering coefficients and phase function of a porous medium by a Monte Carlo technique, Int. J. Heat Mass Transfer 47 (2) (2004) 373–383, http://dx.doi.org/10.1016/S0017-9310(03)00146-7 (Available: <http://resolver.scholarsportal.info/resolve/00179310/v47i0002/373_dioaasmbamct>).
[7] J. Petrasch, P. Wyss, A. Steinfeld, Tomography-based Monte Carlo determination of radiative properties of reticulate porous ceramics, J. Quant. Spectrosc. Radiat. Transfer 105 (2) (2007) 180–197, http://dx.doi.org/10.1016/j.jqsrt.2006.11.002.
[8] R. Coquard, D. Baillis, Radiative properties of dense fibrous medium containing fibers in the geometric limit, J. Heat Transfer 128 (10) (2006) 1022–1030, http://dx.doi.org/10.1115/1.2345426.
[9] S. Haussener, P. Coray, W. Lipinski, P. Wyss, A. Steinfeld, Tomography-based heat and mass transfer characterization of reticulate porous ceramics for high-temperature processing, J. Heat Transfer 132 (2) (2010) 023305, http://dx.doi.org/10.1115/1.4000226.
[10] B. Zeghondy, E. Iacona, J. Taine, Determination of the anisotropic radiative properties of a porous material by radiative distribution function identification (RDFI), Int. J. Heat Mass Transfer 49 (17–18) (2006) 2810–2819, http://dx.doi.org/10.1016/j.ijheatmasstransfer.2006.02.034.
[11] B. Zeghondy, E. Iacona, J. Taine, Experimental and RDFI calculated radiative properties of a mullite foam, Int. J. Heat Mass Transfer 49 (19–20) (2006) 3702–3707, http://dx.doi.org/10.1016/j.ijheatmasstransfer.2006.02.036.
[12] N.J. Dyck, A.G. Straatman, A new approach to digital generation of spherical void phase porous media microstructures, Int. J. Heat Mass Transfer 81 (2015) 470–477, http://dx.doi.org/10.1016/j.ijheatmasstransfer.2014.10.017.
[13] D. Baillis, M. Raynaud, J.F. Sacadura, Determination of spectral radiative properties of open cell foam: model validation, J. Thermophys. Heat Transfer 14 (2) (2000) 137–143, http://dx.doi.org/10.2514/2.6519.
[14] D.P. Anderson, P.G. Wapner, D.B. Curliss, Physical property characteristics of pitch materials, Presented at MRS Proceedings, 1992.
[15] Dassault Systemes, Solidworks Educational Version 2012–2013.